






Low-energy electron-induced decomposition of 5-trifluoromethanesulfonyl-uracil: A potential radiosensitizer

Cite as: J. Chem. Phys. **149**, 164307 (2018); <https://doi.org/10.1063/1.5050594>

Submitted: 01 August 2018 . Accepted: 05 October 2018 . Published Online: 29 October 2018

J. Ameixa , E. Arthur-Baidoo, R. Meißner , S. Makurat , W. Kozak , K. Butowska, F. Ferreira da Silva , J. Rak, and S. Denifl



View Online



Export Citation



CrossMark

ARTICLES YOU MAY BE INTERESTED IN

Electron attachment to gas-phase uracil

The Journal of Chemical Physics **120**, 6557 (2004); <https://doi.org/10.1063/1.1649724>

Doubly charged coronene clusters—Much smaller than previously observed

The Journal of Chemical Physics **148**, 174303 (2018); <https://doi.org/10.1063/1.5028393>

Resonant electron attachment to mixed hydrogen/oxygen and deuterium/oxygen clusters

The Journal of Chemical Physics **147**, 194301 (2017); <https://doi.org/10.1063/1.5003428>

Lock-in Amplifiers

Find out more today



Zurich
Instruments



Low-energy electron-induced decomposition of 5-trifluoromethanesulfonyl-uracil: A potential radiosensitizer

J. Ameixa,^{1,2,a)} E. Arthur-Baidoo,¹ R. Meißner,^{1,2} S. Makurat,³ W. Kozak,³ K. Butowska,⁴ F. Ferreira da Silva,² J. Rak,^{3,b)} and S. Denifl^{1,c)}

¹*Institut für Ionenphysik und Angewandte Physik and Center for Molecular Biosciences (CMBI), Leopold-Franzens Universität Innsbruck, Technikerstraße 25/3, 6020 Innsbruck, Austria*

²*Laboratório de Colisões Atômicas e Moleculares, CEFITEC, Departamento de Física, Faculdade de Ciências e Tecnologia, Universidade NOVA de Lisboa, Campus de Caparica, 2829-516 Caparica, Portugal*

³*Laboratory of Biological Sensitizers, Physical Chemistry Department, Faculty of Chemistry, University of Gdańsk, 80-308 Gdańsk, Poland*

⁴*Laboratory of Biophysics, Department of Molecular and Cellular Biology, Intercollegiate Faculty of Biotechnology of the University of Gdańsk and Medical University of Gdańsk, 80-307 Gdańsk, Poland*

(Received 1 August 2018; accepted 5 October 2018; published online 29 October 2018)

5-trifluoromethanesulfonyl-uracil (OTfU), a recently proposed radiosensitizer, is decomposed in the gas-phase by attachment of low-energy electrons. OTfU is a derivative of uracil with a triflate (OTf) group at the C₅-position, which substantially increases its ability to undergo effective electron-induced dissociation. We report a rich assortment of fragments formed upon dissociative electron attachment (DEA), mostly by simple bond cleavages (e.g., dehydrogenation or formation of OTf⁻). The most favorable DEA channel corresponds to the formation of the triflate anion alongside with the reactive uracil-5-yl radical through the cleavage of the O–C₅ bond, particularly at about 0 eV. Unlike for halouracils, the parent anion was not detected in our experiments. The experimental findings are accounted by a comprehensive theoretical study carried out at the M06-2X/aug-cc-pVTZ level. The latter comprises the thermodynamic thresholds for the formation of the observed anions calculated under the experimental conditions (383.15 K and 3×10^{-11} atm). The energy-resolved ion yield of the dehydrogenated parent anion, (OTfU–H)⁻, is discussed in terms of vibrational Feshbach resonances arising from the coupling between the dipole bound state and vibrational levels of the transient negative ion. We also report the mass spectrum of the cations obtained through ionization of OTfU by electrons with a kinetic energy of 70 eV. The current study endorses OTfU as a potential radiosensitizer agent with possible applications in radio-chemotherapy. *Published by AIP Publishing.* <https://doi.org/10.1063/1.5050594>

I. INTRODUCTION

Regardless of the noticeable effort in finding and improving anticancer therapies, radiotherapy is still one of the prevailing strategies to defeat cancer. However, hypoxia is the *Achilles heel* of radiotherapy, which significantly decreases the efficiency of such therapy in hypoxic tumors.¹ The concomitant application of radiotherapy with chemotherapeutic drugs, namely, radiosensitizers, represents thus an alternative as well as more efficient type of therapy. An ideal radiosensitizer selectively binds to tumor cells which enhances their radiosensitivity² and results in the reduction of the administered dose of radiation, ultimately leading to little or no effect to healthy cells. In fact, incorporation of an electrophilic substituent into DNA substantially enhances its radiosensitivity

toward high-energy radiation, without altering gene expression prior to irradiation.^{3–5} For instance, a uracil derivative with an electrophilic group (e.g., halogen) in the C₅-position has been extensively used as radiosensitizers^{5,6}—such compounds are known as 5-halouracils. However, in spite of the intensive research devoted to this subject, the fundamental reactions underlying the operation of such compounds are still unclear. Nevertheless, it is acknowledged that in the physicochemical stage of radiation damage the reactivity of such compounds to low-energy electrons plays a crucial role in the sensitization process notably through dissociative electron attachment (DEA) reactions.⁷ In brief, the interaction of high-energy radiation with a biological medium yields low-energy (<20 eV) electrons (LEEs), at a number of 10⁴/MeV of incident radiation.⁸ Thereafter, these LEEs are thermalized, within the picosecond time scale, to subexcitation energies, thereby generating highly reactive species, namely, OH[•] and H[•] which may also react further with DNA.⁹ However, prior to thermalization, radiosensitizer molecules, which are present in the biological medium, may capture these LEEs

^{a)}E-mail: j.ameixa@campus.fct.unl.pt

^{b)}E-mail: janusz.rak@ug.edu.pl

^{c)}E-mail: stephan.denifl@uibk.ac.at

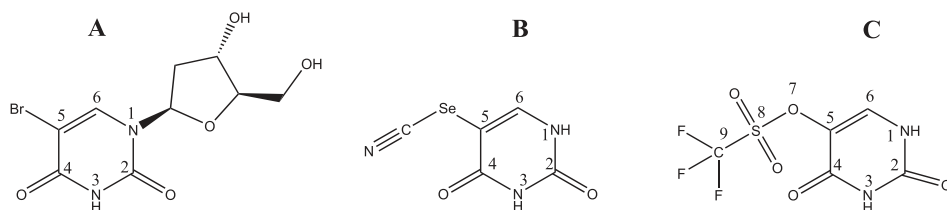


FIG. 1. Structures of (a)—5-bromo-2'-deoxyuridine (5-BrdU), (b)—5-selenocyanatouracil (SeCNU), and (c)—5-trifluoromethanesulfonyl-uracil (OTfU).

and then undergo DEA, particularly at energies below the threshold for electronic excitation. Therefore, an effective radiosensitizer must be decomposed efficiently upon electron attachment, thus generating reactive radicals (i.e., uracil-yl) which may react with DNA, leading to the loss of integrity of such a key biomolecule.⁶ Notably, the interaction of LEEs with 5-halouracils in the gas phase has been comprehensively studied experimentally as well as by theoretical methods.¹⁰ In particular, such studies have been carried out for 5-chlorouracil,^{11–16} 5-fluorouracil,^{11,14–16} 5-iodouracil,^{11,17} and 6-chlorouracil.^{13,15} Electron transfer from potassium atoms to 5-fluorouracil and 5-chlorouracil has been assessed as well.¹⁸ To our best knowledge, 5-bromo-2'-deoxyuridine (5-BrdU), shown in Fig. 1(a), is the most comprehensively studied radiosensitizer.^{19,20} Consequently, there is an urgent need for new and more efficient compounds with radiosensitizing properties. A methodology concerning the proposal of new radiosensitizers was suggested,⁶ in addition to several analogs proposed by Rak and co-workers.⁵ The most efficient compound turned out to be 5-selenocyanatouracil (SeCNU), shown in Fig. 1(b), which is 1.5-fold more effectively decomposed by solvated electrons when compared to BrU.²¹ In the light of such findings, a novel compound was proposed—5-trifluoromethanesulfonyl-2'-deoxyuridine (OTfU). It possesses a substantial adiabatic electron affinity (AEA) and appears to be prone to undergo effective electron-induced dissociation,²² thereby can be treated as a pseudohalouracil. Its fragmentation induced by solvated electrons was studied by steady-state radiolysis combined with theoretical methods.²² However, no DEA study in the gas-phase has been reported so far. Therefore, we have investigated DEA to 5-trifluoromethanesulfonyl-uracil (OTfU), shown in Fig. 1(c), in the gas-phase in order to unravel the fundamental dissociation channels induced by LEEs. Moreover, the mass spectrum of cations formed via dissociative electron ionization at the electron energy of ~ 70 eV is also presented in order to study the fragmentation pathways upon positive ion formation. Finally, the observed DEA reactions were studied by theoretical calculations; in particular, the respective thermodynamic thresholds as well as the AEA for the observed anions and the neutral OTfU molecule were calculated.

II. METHODS

A. Dissociative electron attachment

The experiments were performed in a crossed electron-molecular beam apparatus coupled with a quadrupole mass spectrometer available at the Innsbruck laboratory, described

in detail previously.²³ The molecular effusive beam is produced by the evaporation of the solid sample in a resistively heated oven inside the vacuum chamber. Then it effuses into the interaction chamber of the hemispherical electron monochromator (HEM) through a capillary of 1 mm diameter where it intersects orthogonally with a monochromatized electron beam. The HEM was shown to generate an electron beam with an energy resolution around 35 meV at full width at half-maximum (FWHM). In the present experiment, an energy resolution of 100 meV (FWHM) was set, which is a suitable compromise between energy resolution and beam intensity. The anions resulting from the electron attachment process are extracted from the interaction chamber by a weak electrostatic field into a quadrupole mass spectrometer where they are mass-analyzed and further detected by a channeltron electron multiplier in single pulse-counting mode. For a given anion, the ion yield is recorded as a function of the electron energy. In order to record a mass spectrum, the electron energy is kept constant and the ion yield is recorded as a function of the mass. The electron energy scale and energy resolution are determined by measuring the well-known ion yields for the formation of $\text{SF}_6^-/\text{SF}_6$ or Cl^-/CCl_4 at 0 eV. The remaining electrons, which crossed the interaction region, are collected in a Faraday plate and monitored using a picoammeter.

B. Synthesis of 5-trifluoromethanesulfonyl-uracil

The compound was obtained via the procedure described by Crisp and Flynn.²⁴ To the solution of 5-hydroxyuracil (75 mg, 0.59 mmol) in pyridine (2 ml), N-phenyltriflimide (251 mg, 0.70 mmol) was added (Fig. 2). The mixture was stirred overnight at room temperature. After concentration under vacuum, the resulting residue was purified by column chromatography using hexane:AcOEt 1:1 as an eluent to give the desired product in a 66.3% yield.

¹H NMR (Bruker AVANCE III, 500 MHz, DMSO), δ : 11.9 (s, 1H), 11.5 (s, 1H), 8.26 (d, 1H); ³C NMR (125 MHz, DMSO), δ : 158.7, 150.5, 133.2, 126.5, and 118.5 (q);

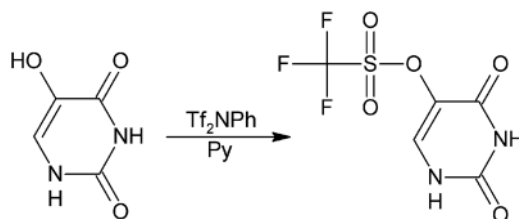


FIG. 2. Synthetic route for 5-OTfU.

HRMS (TripleTOF 5600+, SCIEX), m/z : $[M-H]^-$ calcd for $C_5H_3F_3N_2O_5S$ 258.9642, found 258.9547. For the MS, 1H and ^{13}C NMR spectra see Figs. S1–S3 in the [supplementary material](#).

C. Computational

In order to achieve a more comprehensive knowledge about the DEA process, a set of theoretical calculations was performed at the M06-2X²⁵/aug-cc-pVTZ^{26,27} level of theory, which has proven to give comparable results to the G4²⁸ extrapolation scheme.²⁹ However, the latter method is much more computationally demanding. In particular, the thermodynamic thresholds of various DEA reactions as well as the AEA of the neutral OTfU and of the observed anions were calculated. Additionally, the dipole-bound states (DBS) of OTfU were predicted. All the calculations were performed with the Gaussian09 suite³⁰ and the visualizations with the VMD package.³¹

1. Thermodynamic thresholds

The thermodynamic threshold for the DEA reactions was calculated as a difference, ΔG , between the Gibbs free energies of reactants in their ground state [Eq. (1)], as it was performed in the previous studies³²

$$\Delta G = G_{products} - G_{substrate}. \quad (1)$$

The substrate was the neutral OTfU [see Fig. 1(c)], and the products consisted of both the anion and radical formed after electron-induced dissociation. The lowest-energy geometry resulted from the conformational scan for the neutral. First, the structures were optimized at the M06-2X/aug-cc-pVTZ level of theory (0 K). Afterwards, in order to obtain thermochemical characteristics (free energies of reactions), the frequency calculations were performed at the same level, both in the standard state (298.15 K, 1 atm) and in the experimental conditions (383.15 K, 3×10^{-11} atm). The pressure correction to the G value for the experimental pressure was obtained using [Eq. (2)],

$$G_{3 \times 10^{-11} \text{ atm}, T} = G_{1 \text{ atm}, T} + TS_{trans; 1 \text{ atm}, T} - TS_{trans; 3 \times 10^{-11} \text{ atm}, T}, \quad (2)$$

where $G_{p,T}$ is the free enthalpy at the pressure p and temperature T and $TS_{trans;p,T}$ denotes the product of temperature and translational entropy at the pressure p and temperature T .³³

Furthermore, the AEA was calculated for OTfU and the anionic products as the free energy difference between the optimized pairs of the neutral and its corresponding anion [Eq. (3)]. For some of the products, the neutral was unstable; therefore, the vertical detachment energy (VDE) was calculated [Eq. (4)],

$$AEA = E_{neut,geom:neut} - E_{anion,geom:anion}, \quad (3)$$

$$VDE = E_{neut,geom:anion} - E_{anion,geom:anion}. \quad (4)$$

2. Conformational scan

The conformational scan was performed with the use of the M06-2X/aug-cc-pVTZ constrained optimizations. Two

dihedral angles $\varphi_{C6-C5-O7-S8}$ and $\varphi_{C5-O7-S8-C9}$ [for atoms numbering see Fig. 1(c)] were systematically changed in steps of 30° to perform a scan of the conformational PES. The lowest-energy points were further subjected to further unconstrained geometry optimizations at the same level of theory and the difference in their Gibbs free energies allowed us to calculate the composition of the gas-phase equilibrated mixture under the experimental conditions. The details and results concerning the conformational scan are provided in the [supplementary material](#).

3. Dipole-bound states

In order to provide the excess electron binding energy for the dipole-bound state (DBS) of OTfU, the neutral conformers (see Fig. S4 of the [supplementary material](#)) of the neutral molecule were first optimized at the MP2/aug-cc-pVTZ level of theory.³⁴ Two of them converged to the same conformations, thus only two neutral conformations exist at the MP2 level. The standard aug-cc-pVTZ basis set was then supplemented with the diffuse functions necessary to describe the diffuse character of the loosely bound electron.³⁵ These basis set functions, centered on the C_6 atom as suggested by the position of the dipole moment vector [for numbering see Fig. 1(c)], were subsequently added with a geometric progression ratio equal to 5.³⁶ The exponent was built up for each symmetry starting from the lowest exponent in the original basis set;³⁷ i.e., the first additional s symmetry was built from the lowest exponent of s symmetry included in the aug-cc-pVTZ basis set for carbon, the second extra s function was equal to the 1/5 of the first function added, and so on. A 5s4p3d2f set of diffuse functions was sufficient to obtain a saturated basis set. Indeed, addition of the further set of diffuse functions extending the space of diffuse atomic orbitals to 6s5p4d3f increases the VEA calculated at the MP2 level by less than 1 cm^{-1} . Therefore, we set up at aug-cc-pVTZ augmented with 5s4p3d2f diffuse functions centered at the C_6 atom to characterize the respective dipole-bound states.

The two-electron integrals were calculated with the accuracy of 10^{-20} (default 10^{-12}), and the full accuracy was switched on during the SCF procedure.³⁸ Thereafter, the vertical electron binding energy was calculated, first, at Koopman's theorem (KT) level as E_{bind}^{KT} , equal to the negative energy of the LUMO orbital of the neutral, and then, supplemented with the orbital relaxation and electron correlation contributions (VEA^{MP2}). Similarly, the adiabatic electron affinity, AEA^{MP2}, was calculated at the MP2 level.

III. RESULTS AND DISCUSSION

A. Formation of cations through dissociative ionization of OTfU

Figure 3 shows the electron ionization mass spectrum of OTfU measured at the electron energy of about 70 eV. To the best of our knowledge, the formation of cations upon dissociative ionization has not been reported so far. We recorded different mass spectra at different oven temperatures (not shown here) in order to achieve a suitable ion yield as well as to rule out thermal decomposition of the compound. It is worth

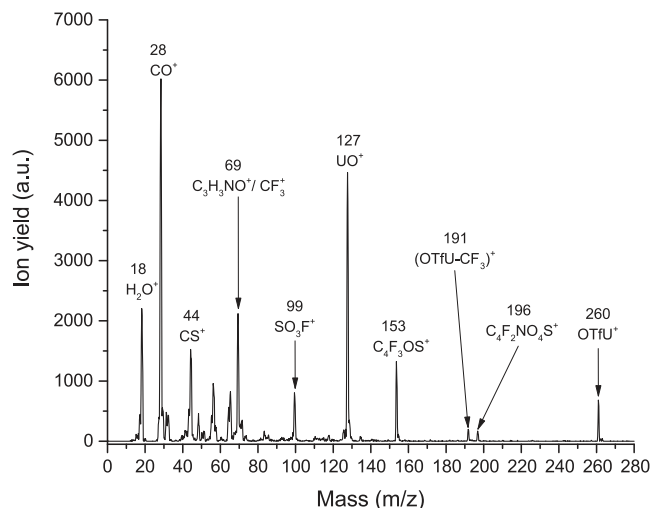
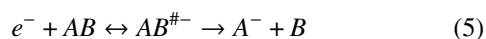


FIG. 3. Mass spectrum of cations formed by electron ionization of OTfU at the electron energy of 70 eV. The oven temperature was set to 383.15 K.

noting that the reported relative ion yields depend on the transmission of the quadrupole mass spectrometer as well as the ion collection efficiency of the cations formed with high initial kinetic energy. The ion at m/z 18 arises from residual water present in the vacuum chamber during the measurements. The cation with the highest yield is CO^+ (m/z 28). Another highly abundant cation is UO^+ (m/z 127) formed by the cleavage of the S–O bond in the triflate group. At m/z 69, two isobaric fragment ions may be present, $\text{C}_3\text{H}_3\text{NO}^+$ and CF_3^+ . They represent the mass peak with the third highest yield. $\text{C}_3\text{H}_3\text{NO}^+$ is the dominant fragment ion upon electron ionization of uracil.³⁹ The complementary cation of CF_3^+ formed by cleavage of the C–S bond within the triflate group, $(\text{OTfU}-\text{CF}_3)^+$ (m/z 191), appears with minor abundance in the mass spectrum. The cations at m/z 153 and m/z 196 are possibly $\text{C}_4\text{F}_3\text{OS}^+$ and $\text{C}_4\text{F}_2\text{NO}_4\text{S}^+$, respectively, which only form by complex rearrangements involving the molecule. The intact parent cation at m/z 260 is also observed. Compared to electron ionization of uracil studied with the same setup,³⁹ one may conclude that the formation of NCO^+ is substantially reduced by the substitution of uracil at the C_5 position with the triflate group.

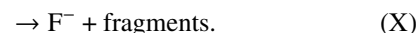
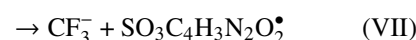
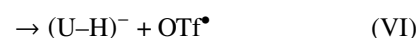
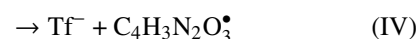
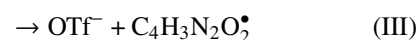
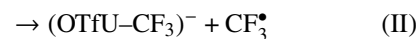
B. Formation of anions upon dissociative electron attachment to OTfU

In general, DEA is a resonant two-step process characterized by the capture of an electron by a molecule AB forming a transient negative ion (TNI), $\text{AB}^{\#-}$. The TNI is formed through a vertical transition (following the Franck-Condon principle) from the ground state of the molecule to an accessible excited state of the anionic molecule, $\text{AB}^{\#-}$. Consequently, the electronically and/or vibrationally excited TNI can relax through several fragmentation channels leading to the formation of an anionic fragment and a neutral fragment [DEA, Eq. (5)],



or via emission of the excess electron thus leaving the molecule in an excited state (autodetachment).

We studied DEA to OTfU in the energy range from about 0 to 14 eV. The following dissociation channels were detected within the experimental detection limit:



The ion yields for all anions detected are discussed in Secs. III B 1–III B 5. To our surprise, the stable parent anion OTfU^- is not observed within the experimental detection limits. Most halonucleobases XU ($X = \text{Cl}, \text{Br}, \text{I}$) do form a stable parent anion upon attachment of a free electron in the gas phase,^{4,12,40–43} in contrast to fluorinated derivatives,⁴⁴ unsubstituted DNA bases,^{45–47} and amino acids.^{48,49} The stabilisation of the parent anion is associated with the positive EA. In fact, the calculated AEA of OTfU at the M06-2X/aug-cc-pVTZ level is about 0.90 eV which is remarkably higher when compared to the AEA calculated by Li *et al.* for particular 5-halouracils (5-XU),⁵⁰ i.e., $\text{EA}(5\text{-FU}) = 0.48$ eV, $\text{EA}(5\text{-ClU}) = 0.60$ eV, and $\text{EA}(5\text{-BrU}) = 0.63$ eV. Therefore, assuming that the metastable parent anion of OTfU is formed, the TNI will be vibrationally excited such that the decay will occur on sub- μs time scales by autodetachment or through the DEA reactions (I)–(X) invalidating its detection. The resonance position for the observed anions, the respective thermodynamic thresholds, as well as the predicted AEA compared to other values available in the literature are summarized in Table I (and for more calculation data, see Table SI in the supplementary material).

1. Dehydrogenated parent anion ($\text{OTfU}-\text{H}^-$)

The ion yield for the formation of the closed shell anion $(\text{OTfU}-\text{H})^-$ is represented by reaction (I). The peak positions for the corresponding resonances are listed in Table I. The formation of the closed shell anion $(\text{OTfU}-\text{H})^-$ mainly occurs through the attachment of electrons with energy well below the threshold for electronic excitation. The anion yield exhibits a rich structure consisting of a set of peaks observed at about $\sim 0, 0.24, 0.56, 0.95,$ and 1.28 eV, as shown in Fig. 4. The formation of the first three sharp peaks (the one at ~ 0 eV is not resolved) may be assigned as vibrational Feshbach resonances (VFR) arising from the vibrational levels of the TNI or from a dipole-bound state (DBS) where an incoming electron may be temporally bounded. Indeed, the dipole moment of the most stable conformer (Fig. S5–A) of the neutral OTfU is estimated to be 3.2 D, while for the second conformer (Fig. S5–B) a considerably higher

TABLE I. Mass for each anion formed upon DEA to OtfU with the respective resonance position, the respective experimental threshold as well as thermodynamic threshold calculated at the M06-2X/aug-cc-pVTZ level (383.15 K, 3×10^{-11} atm) and the predicted adiabatic electron affinity compared to other values available in the literature. The AEA of OtfU is 0.9 eV at M06-2X/aug-cc-pVTZ.

Mass (m/z)	Anion	Resonance position (eV)					Threshold (eV)		AEA (eV)	
		1	2	3	4	5	Exp.	Calc.	Calc.	Lit.
259	[OtfU-H] ⁻	~0	0.24	0.56	0.95	1.28	~0	N ₁ -H -1.05 ^a	4.19	...
								N ₃ -H -0.56 ^a	4.70	...
								C ₆ -H -0.01 ^a	3.67	...
191	[OtfU-CF ₃] ⁻	~0	2.53	~0	-3.09 ^a	4.02 ^b	...
149	OTf ⁻	~0	0.14	1.05	3.65	...	~0	-2.44 ^a	6.22 ^b	5.50 ^c
133	Tf ⁻	~0	0.13	1.04	3.60	...	~0	-3.22 ^a	3.61	...
127	[OtfU-CF ₃ SO ₂] ⁻ /OU ⁻	~0	0.13	1.07	~0	-2.00 ^a	2.38	...
111	[OtfU-CF ₃ SO ₃] ⁻ /[U-H] ⁻	~1.2	~0.2	1.25	2.26	2.34 ^d
69	CF ₃ ⁻	~0	2.35	4.75	8.45	...	~0	-0.74 ^a	1.69	2.01 ^e
64	SO ₂ ⁻	~0	~0	-3.92 ^a	1.42	1.11 ^e
42	NCO ⁻	~0	~1.8	~4.0	~8.1	...	~0
19	F ⁻	~4.8	~8.0	~3.1	0.61	3.27	3.40 ^e

^aThe negative value obtained from the calculations corresponds to the experimental threshold of 0 eV.

^bThe neutral product is unstable. AEA is calculated for the neutral geometry with the frozen bond that is prone to break. Additionally VDE was calculated for both anions. $VDE_{[OtfU-CF_3]^-} = 4.47$ eV and $VDE_{[CF_3SO_2]^-} = 6.67$ eV.

^cData taken from Refs. 51 and 52.

^dData taken from Ref. 50, i.e., AEA(Ur-5-y1*).

^eData taken from Ref. 53.

dipole moment of 5.4 is predicted at the M06-2X/aug-cc-pVTZ level of theory. These values are above the critical value (2.0–2.5 D)⁵⁴ required for the existence of a dipole-bound state (DBS).

In Fig. 5, the characteristic distributions of the SOMO orbital for DBSs formed by both conformers are depicted. As indicated by the numbers gathered in Table II, the anion originated from conformer A, of smaller dipole moment, is bound by only 9 meV at the KT level, while the more polar structure forms DBS characterized by the KT vertical energy attachment of 47 meV. Electron correlation is significant for DBSs since dipole moment is seriously overestimated at the HF level.

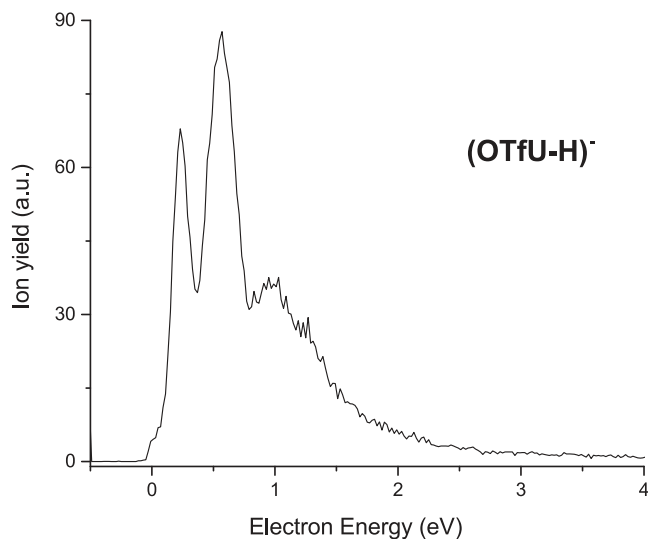


FIG. 4. Ion yield of (OtfU-H)⁻ formed upon DEA to OtfU.

On the other hand, dynamic correlation stabilizes DBSs to a large extent. Although these two effects have opposite signs, they usually do not cancel out which makes the calculations at the correlated level obligatory.⁵⁵ Actually, the VEA^{MP2} values gathered in Table II constitute a good illustration of the mentioned above (9 vs. 39 and 47 vs. 97 meV for conformation A and B, respectively; see Table II). An additional stabilization of DBS results from geometry relaxation due to anion formation. However, since the excess electron density of DBS is beyond the molecular framework (see Fig. 5), this effect, unlike for valence bound anions, is relatively small, cf. VEA^{MP2} with AEA^{MP2} (Table II).

Therefore, the coupling between the vibrational levels of the TNI with DBSs may arise as an effective DEA channel leading to the dehydrogenation of OtfU. In fact, DBS for the most abundant conformation of OtfU was predicted to lie 54 meV below the neutral (see Table II). Concerning the second conformer (Fig. 5), its DBS lies as much as 110 meV (see Table II) lower than the neutral. Notably, the same mechanism involving DBS underlying the dehydrogenation of uracil and thymine upon attachment of electrons with an energy below 3 eV has been proposed by a combination of experimental and theoretical methods.⁵⁶ In the case of OtfU, different anionic isomers may form by dehydrogenation depending on the site of H-loss—N₁, N₃, or C₆ in the uracil moiety. As so, the variation of the Gibbs free energy for each possible isomer is listed in Table I. The thermodynamic calculations show that in spite of the dehydrogenation site, the loss of a hydrogen from OtfU is always an exothermic reaction, whereas the dehydrogenation from the N₁ position appears to be thermodynamically most favorable. Note that the energetically most favorable loss of hydrogen upon DEA to uracil occurs from the N₁ position as well.^{56,57} Furthermore, the predicted AEA for (OtfU-H)⁻

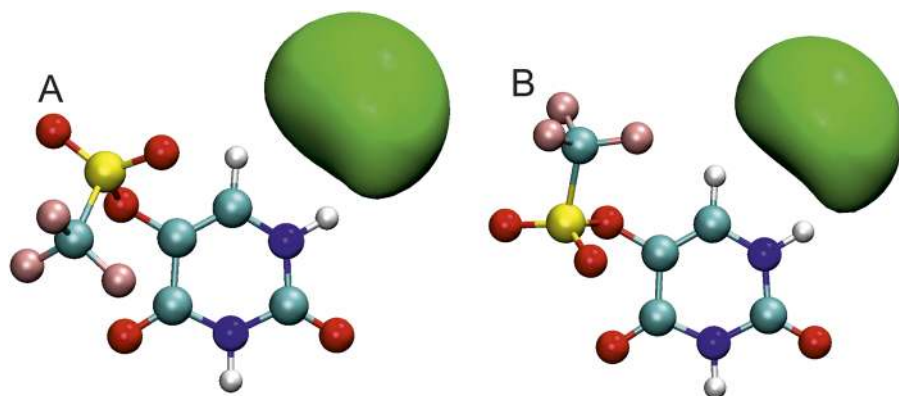


FIG. 5. The SOMO orbitals of the anions for both conformers considered. The isosurface value for the most stable conformer (a) is $0.001 \text{ a.u.}^{-3/2}$, while the second one (b) is equal to $0.018 \text{ a.u.}^{-3/2}$.

depends on the dehydrogenation site, and it varies from 3.67 to 4.19 eV, as shown in Table I.

2. Cleavage of the C–S bond in the triflate group

The cleavage of the C–S bond within the triflate group leads to the formation of two complementary anions with the ion yields shown in Fig. 6. First, $(\text{OTfU}-\text{CF}_3)^-$ is formed via reaction (II) where the trifluoromethyl radical ($-\text{CF}_3^\bullet$) is formed as a neutral byproduct. The experimental threshold of about 0 eV is in agreement with the calculated thermochemical threshold of -3.09 eV . The AEA of $(\text{OTfU}-\text{CF}_3)^-$ is predicted to be 4.02 eV. However, the trifluoromethyl radical appears to be unstable. Second, the closed shell anion CF_3^- is formed via the complementary reaction (VII) together with $(\text{OTfU}-\text{CF}_3)^\bullet$. The respective experimental threshold is also about 0 eV, which matches with the calculated thermochemical threshold of -0.74 eV . The theoretical AEA of 1.69 eV for CF_3^- is comparable to the AEA of 2.01 eV obtained by photoelectron spectroscopy reported in the literature.⁵³ In addition to a strong resonance near 0 eV for the former anion and hardly present for the latter anion, the ion yields of $(\text{OTfU}-\text{CF}_3)^-$ as well as CF_3^- exhibit a broad resonance centered at about 2.4 eV. The anion yield of CF_3^- further exhibits a resonance at 4.75 eV and a broad structure at 8.45 eV. The presence of a resonance for both anions at the same positions, i.e., about 2.4 eV, is the evidence that the formation of both species may occur from a common electronic state of the TNI. The formation of the aforementioned anions was previously reported by Ptasińska *et al.* in DEA studies with the triflate analogs in the gas-phase.⁵² In brief, they reported the formation of the counterpart of the $-\text{CF}_3^\bullet$ radical through resonances near 0 eV and 2.5–3.0 eV electron energies for the triflates containing a phenyl ring and only at 3 eV for the methyl triflate. Notably, a good agreement is observed between the resonance positions

TABLE II. Electron binding characteristics for dipole bound states supported by conformers A and B. All values shown in meV.

	Conformer A	Conformer B
$E_{\text{bind}}^{\text{KT}}$	9	47
VEA^{MP2}	39	97
AEA^{MP2}	54	110

that lead to the formation of $(\text{OTfU}-\text{CF}_3)^-$ by C–S bond cleavage either in OTfU or in triflate analogs. Therefore, one may conclude, based on this similarity, that the uracil ring attached to the triflate in OTfU has little effect on the electron energies required to cleave the C–S bond within the triflate. On the other hand, the formation of CF_3^- in the triflate analogs occurs mainly through a resonant state at 3 eV in addition to other states located at higher electron energies which depend on the considered analog, i.e., at 8 eV for methyl triflate and at 6 and 7.5 eV for tolyl triflate. In the present study, CF_3^- is formed from OTfU by the same number of resonant states such as in tolyl triflate, even though the respective positions appear to be different.

3. Cleavage of the O–S bond in the triflate group versus cleavage of the O–C₅ bond in the uracil group

The triflate (OTf^-) and triflyl (Tf^-) anions are formed upon a simple bond cleavage, i.e., the O–C₅ bond within the triflate group and the O–S bond in uracil and they are represented by reactions (III) and (IV), respectively. The calculations show that the neutral by-product, $\text{C}_4\text{H}_3\text{N}_2\text{O}_2^\bullet$, which is formed alongside OTf^- appears to be unstable. These two DEA

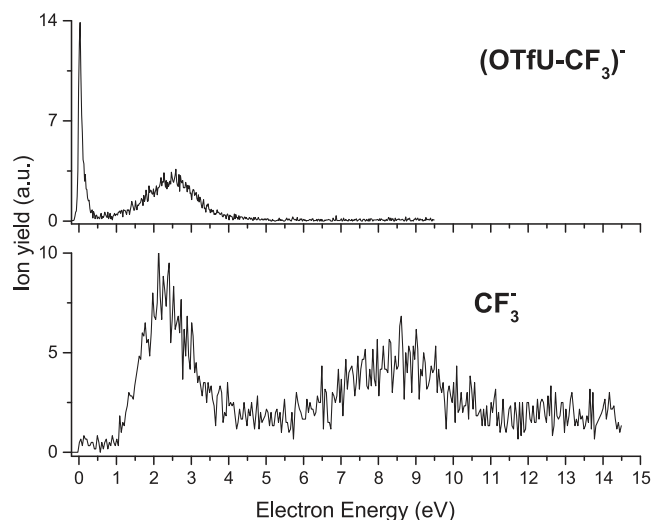


FIG. 6. Ion yield of $(\text{OTfU}-\text{CF}_3)^-$ and CF_3^- formed by the cleavage of the C–S bond within the triflate upon DEA to OTfU.

reactions represent the most favorable fragmentation channels, particularly close to 0 eV. Further resonances at about 0.13 eV, 1.05 eV, and at around 3.65 eV were observed as well for both anions (see Fig. 7). Such finding is in line with the outcomes of the DEA^{4,41} and theoretical¹⁷ studies with 5-BrU, where the abstraction of the halide anion Br⁻ represents the main dissociation pathway. The highly exothermic character is not surprising though since the anionic products possess a large AEA, i.e., AEA(Tf) = 3.61 eV and AEA(OTf) = 6.22 eV (see Table I). The calculated thermochemical thresholds of -2.44 eV for the formation of OTf⁻ and -3.22 eV for the formation of Tf⁻ are in good agreement with the peaks at about 0 eV obtained experimentally. However, Ptasińska *et al.* reported an energy barrier of about 0.5 eV for the formation of OTf⁻ through DEA to triflate analogs,⁵² which is not observed in the present study. The predicted AEAs of about 6.22 eV for the triflate group and about 3.61 eV for the triflyl group represent the driving forces of these DEA reactions. Albeit, to our best knowledge, the AEA of the triflyl group is not reported in the literature. Under the same experimental conditions, the intensity of the triflate anion is higher when compared to the intensity of the triflyl anion, which may suggest that the O-C₅ bond is more readily cleaved than the O-S bond within the triflate group. These findings can be compared with the outcomes obtained by Makurat *et al.* upon electron attachment in an aqueous 5-trifluoromethanesulfonyl-2'-deoxyuridine (OTfdU) solution.²² Briefly, this study was carried out in a deoxygenated aqueous OTfdU solution containing an OH[•] radical scavenger and phosphate buffer (pH = 7.0). Solvated electrons were generated in the solution through irradiation with X-rays. Thereafter, the products formed by electron attachment to OTfdU were probed by liquid chromatography mass spectrometry (LC-MS) operated in the negative mode. The authors reported that in the experiment the most abundant dissociation channel leads to the formation of dU by the cleavage of the C₅-O bond in the triflate group, in opposition to calculations, which indicated that in solution the O-S bond cleavage would be thermodynamically more

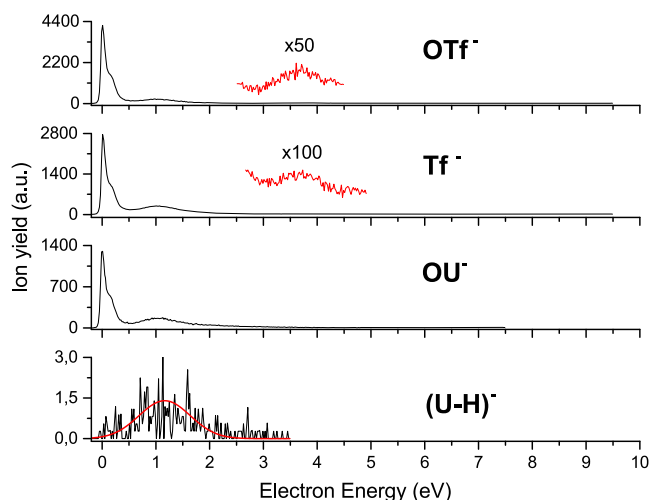


FIG. 7. Ion yield of OTf⁻, Tf⁻, OU⁻, and (U-H)⁻ formed either by the cleavage of the S-O bond or the O-C₅ bond in the uracil upon DEA to OTfU. The ion yield for (U-H)⁻ can be likely ascribed to a weak impurity since the resonance is below the calculated threshold for the DEA reaction (VI).

favorable. This discrepancy was finally explained by protonation of the compound at the C₅ position in solution which promotes the cleavage of the C₅-O bond rather than the O-S bond.²² The present calculations for the gas phase also predict that the cleavage of the O-S bond should be more favorable (see Table I); however, the total ion yields for cleavage of the C₅-O bond vs. the O-S bond are approximately equal. In this context, we note that under single collision conditions, the yield of a particular anion formed by DEA is associated to the DEA cross section σ_{DEA} , which is influenced by autodetachment. This situation is expressed by

$$\sigma_{DEA} = \sigma_0 P_{diss}, \quad (6)$$

where σ_0 represents the electron attachment cross section and P_{diss} represents the dissociation probability which is a function of the autodetachment lifetime, τ_{AD} , and the dissociation time, τ_{DEA} , as follows:

$$P_{diss} = \exp\left(-\frac{\tau_{DEA}}{\tau_{DA}}\right). \quad (7)$$

Thus, despite the inferior thermodynamic threshold for the cleavage of the O-S bond within the triflate group leading to the formation of Tf⁻, it does not imply that the formation of this particular anion should be favored over the formation of OTf⁻ upon cleavage of the O-C₅ bond in uracil.

In addition to reactions (III) and (IV), which lead to the formation of negatively charged triflate and triflyl ions, we report the formation of OU⁻ upon cleavage of the O-S bond within the triflate group, represented by reaction (V), mainly through a resonance at about 0 eV as well as others at 0.13 and 1.07 eV (see Fig. 7). The experimental threshold of about 0 eV is in accordance with the predicted thermodynamic threshold of -2.00 eV. The reaction (VI) represents the formation of dehydrogenated uracil, (U-H)⁻, upon cleavage of the O-C₅ bond in uracil, which is endothermic and characterized by the predicted thermodynamic threshold of about 1.25 eV. This dissociation channel appears to be unfavorable in the experiment, with a very low intensity of the ion yield as shown in Fig. 7. The experimental onset of ~0.2 eV was obtained, which is lower than the theoretical threshold and thus indicating rather an impurity.

Finally, we note that the energy-resolved ion yields regarding the above mentioned DEA reactions (III)-(V) exhibit peaks at the same electron energy, which suggests that the anions may be generated from a common electronic state of the TNI. Moreover, this set of reactions represents a prime example where a particular bond was cleaved, and the negative charge stayed on complementary parts of the molecule.

4. Complex fragmentation pathways: SO₂⁻ and NCO⁻

Apart from single bond cleavages, DEA to OTfU leads to the formation of further anionic species by multiple bond cleavages or through complex rearrangements within the molecule. Namely, the sulphur dioxide (SO₂⁻) anion results from the cleavage of two bonds, i.e., the C-S and the S-O bond in the triflate group, upon attachment of a single electron with 0 eV energy, as represented by reaction (VIII) and shown in Fig. 8. The experimental outcome is in line with the predicted

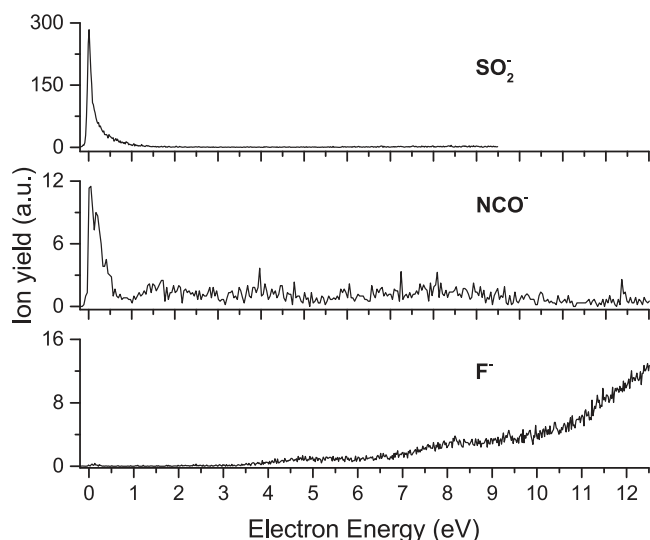


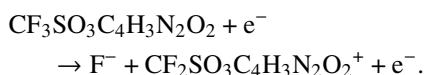
FIG. 8. Ion yields of SO_2^- , NCO^- , and F^- formed upon DEA to OTfU.

thermodynamic threshold for this reaction of about -3.92 eV (Table I). The theoretical AEA of 1.42 eV (Table I) for SO_2^- is comparable to the AEA of 1.11 eV reported in the literature.⁵³ We note that the formation of SO_2^- through DEA to triflate analogs in the gas-phase seems to be a more complex process⁵² since SO_2^- ion yields exhibit resonances at different positions for each analog.

We report the formation of NCO^- by DEA to OTfU as represented by reaction (IX) and shown in Fig. 8. The anion is rather weakly formed in a resonance centered at about 0 eV and even less intense in resonances at energies above 0 eV. Under the present experimental conditions, the ion yield seems to be reduced which hinders the identification of resonances at higher electron energies. It is worth noting that the underlying mechanism regarding the formation of NCO^- upon DEA to pyrimidine bases⁵⁸ and halouracils XU ($X = \text{Cl}, \text{Br}$)^{4,12} has been already intensively investigated in recent years (see Ref. 58). Therefore, we omit a detailed description regarding the formation of this only weakly abundant anion based on quantum chemical calculations for OTfU.

5. Cleavage of the C–F bond in the triflate group: Formation of F^-

The formation of F^- occurs by a single bond cleavage in the triflate group, as represented by reaction (X). The anion yield shows very interesting features resulting from the superimposition of two resonances at about 4.8 and 8.0 eV, which are formed by electron attachment, and a continuous ion signal, which results from the non-resonant ion pair formation process, as shown in Fig. 8. The weak contribution at 0 eV is not due to the DEA reaction, and it may be assigned as an artifact.⁵⁹ The ion pair formation usually occurs at higher electron energies than the DEA process and, in this case, may be described as follows:



The calculated thermodynamic threshold concerning the DEA reaction is 0.61 eV, which is considerably lower than the experimental onset of about 3.2 eV. Therefore, fragmentations, which are more complex, have been further investigated. The thermodynamic thresholds, which lead to the formation of F^- , are presented in Table SII in the [supplementary material](#). The DEA reaction appears to be endothermic in most cases. Notably, the experimental onset lies above the thermodynamic threshold in all cases, which does not allow an unambiguous assignment. Furthermore, the predicted AEA of 3.27 eV for the fluorine anion matches with the value (3.40 eV) reported in the literature.⁵³

IV. CONCLUSION

We studied electron attachment in the gas-phase to the recently synthesized radiosensitizer OTfU in the electron energy range 0 – 14 eV. OTfU may be considered as a pseudo-halouracil. The triflate group present at the C_5 position in the uracil ring possesses a large electron affinity (6.22 eV) which overcomes the electron affinity of all halogens. We observed ten different anionic species formed through DEA to OTfU either upon simple bond cleavage (e.g., formation of OTf^- and loss of H^\bullet) or upon complex reactions (e.g., formation of SO_2^- and NCO^-). In most cases, we observed that an anion and its counterpart are formed by the decay of the same electronic state of the TNI since the ion yields concerning both anions exhibit resonance(s) at similar positions. The best example is represented by the cleavage of the S–O bond in the triflate group leading to the formation of Tf^- and the OU^- as well as by the cleavage of the O– C_5 bond in the uracil leading to the formation of OTf^- through resonant states at similar positions. Moreover, the features presented in the energy-resolved ion yield concerning the loss of H^\bullet were assigned as VFR involving the dipole-bound state of the neutral OTfU. The AEA of the formed anions is comparable to the values previously reported in the literature in most cases.

In contrast to negative ion formation, the stable parent ion can be detected upon electron ionization. Also for this ionization process, reactions accompanied by the cleavage of the S–O bond in the triflate group are dominant. For example, the formation of OU^+ , which is the second most abundant cation observed, is only possible by the cleavage of this bond. However, otherwise the electron ionization mass spectrum shows several abundant cations formed by complex fragmentation reactions.

Ultimately, this study endorses OTfU as a potential radiosensitizer, in particular due to its high reactivity toward low-energy electrons. These LEEs very efficiently decompose OTfU and thereby generate radicals (e.g., uracil-yl) which may further react with DNA. This property is supported by the exothermic character predicted for nine out of eleven calculated DEA reactions, thus operative upon attachment of electrons with about 0 eV.

SUPPLEMENTARY MATERIAL

See [supplementary material](#) for the electrospray ionization mass spectrum of OTfU, the ^1H and ^{13}C NMR spectra

of OTfU, as well as more computational data including conformational scan, dipole-bound states, calculated thresholds at different conditions, and other reaction pathways leading to the formation of the F⁻ anion.

ACKNOWLEDGMENTS

J.A., R.M., and F.F.d.S. acknowledge the Portuguese National Funding Agency FCT–MCTES through Grant Nos. PD/BD/114447/2016 and PD/BD/114452/2016 and researcher position No. IF-FCT IF/00380/2014, respectively, and the research Grant No. UID/FIS/00068/2013. This work was supported by the Radiation Biology and Biophysics Doctoral Training Programme (RaBBiT, PD/00193/2012) and UID/Multi/04378/2013 (UCIBIO). S.D. acknowledges support from FWF (P30332). This work was also supported by the Polish National Science Center (NCN) under the Grant No. UMO-2014/14/A/ST4/00405 (J.R.). The calculations have been carried out in the Wrocław Center for Networking and Supercomputing (wcss.wroc.pl), Grant No. 209 and at a local cluster.

- ¹S. Rockwell, I. Dobrucki, E. Kim, S. Marrison, and V. Vu, *Curr. Mol. Med.* **9**, 442 (2009).
- ²K. Tanzer, L. Feketeová, B. Puschnigg, P. Scheier, E. Illenberger, and S. Denifl, *Angew. Chem., Int. Ed.* **53**, 12240 (2014).
- ³K. Westphal, J. Wiczak, J. Miloch, G. Kciuk, K. Bobrowski, and J. Rak, *Org. Biomol. Chem.* **13**, 10362 (2015).
- ⁴H. Abdoul-Carime, M. A. Huels, F. Brüning, E. Illenberger, and L. Sanche, *J. Chem. Phys.* **113**, 2517 (2000).
- ⁵S. Makurat, L. Chomicz-Mañka, and J. Rak, *ChemPhysChem* **17**, 2572 (2016).
- ⁶L. Chomicz-Mañka, M. Zdrowowiec, F. Kasprzykowski, J. Rak, A. Buonauriguro, Y. Wang, and K. H. Bowen, *J. Phys. Chem. Lett.* **4**, 2853 (2013).
- ⁷Y. Park, K. Polska, J. Rak, J. R. Wagner, and L. Sanche, *J. Phys. Chem. B* **116**, 9676 (2012).
- ⁸S. M. Pimblott and J. A. LaVerne, *J. Phys. Chem. A* **101**, 5828 (1997).
- ⁹E. Alizadeh and L. Sanche, *Chem. Rev.* **112**, 5578 (2012).
- ¹⁰J. D. Gorfinkiel and S. Ptasińska, *J. Phys. B: At., Mol. Opt. Phys.* **50**, 182001 (2017).
- ¹¹H. Abdoul-Carime, M. A. Huels, E. Illenberger, and L. Sanche, *Int. J. Mass Spectrom.* **228**, 703 (2003).
- ¹²S. Denifl, S. Matejcik, B. Gstir, G. Hanel, M. Probst, P. Scheier, and T. D. Märk, *J. Chem. Phys.* **118**, 4107 (2003).
- ¹³S. Denifl, S. Matejcik, S. Ptasińska, B. Gstir, M. Probst, P. Scheier, E. Illenberger, and T. D. Märk, *J. Chem. Phys.* **120**, 704 (2004).
- ¹⁴A. M. Scheer, K. Aflatooni, G. A. Gallup, and P. D. Burrow, *Phys. Rev. Lett.* **92**, 068102 (2004).
- ¹⁵R. Abouaf and H. Dunet, *Eur. Phys. J. D* **35**, 405 (2005).
- ¹⁶F. Kossoski, M. H. F. Bettega, and M. T. d. N. Varella, *J. Chem. Phys.* **140**, 024317 (2014).
- ¹⁷F. Kossoski and M. T. d. N. Varella, *Phys. Chem. Chem. Phys.* **17**, 17271 (2015).
- ¹⁸F. Ferreira da Silva, D. Almeida, R. Antunes, G. Martins, Y. Nunes, S. Eden, G. Garcia, and P. Limão-Vieira, *Phys. Chem. Chem. Phys.* **13**, 21621 (2011).
- ¹⁹B. Djordjevic, *J. Exp. Med.* **112**, 509 (1960).
- ²⁰R. L. Erikson and W. Szybalski, *Radiat. Res.* **20**, 252 (1963).
- ²¹M. Sosnowska, S. Makurat, M. Zdrowowiec, and J. Rak, *J. Phys. Chem. B* **121**, 6139 (2017).
- ²²S. Makurat, M. Zdrowowiec, L. Chomicz-Mañka, W. Kozak, I. E. Serdiuk, P. Wityk, A. Kawecka, M. Sosnowska, and J. Rak, *RSC Adv.* **8**, 21378 (2018).
- ²³S. Denifl, S. Ptasińska, B. Sonnweber, P. Scheier, D. Liu, F. Hagelberg, J. Mack, L. T. Scott, and T. D. Märk, *J. Chem. Phys.* **123**, 104308 (2005).
- ²⁴G. T. Crisp and B. L. Flynn, *Tetrahedron* **49**, 5873 (1993).
- ²⁵Y. Zhao and D. G. Truhlar, *Theor. Chem. Acc.* **120**, 215 (2008).
- ²⁶R. A. Kendall, T. H. Dunning, and R. J. Harrison, *J. Chem. Phys.* **96**, 6796 (1992).
- ²⁷D. E. Woon and T. H. Dunning, *J. Chem. Phys.* **98**, 1358 (1993).
- ²⁸L. A. Curtiss, P. C. Redfern, and K. Raghavachari, *J. Chem. Phys.* **126**, 084108 (2007).
- ²⁹A. Ribar, K. Fink, M. Probst, S. E. Huber, L. Feketeová, and S. Denifl, *Chem. - Eur. J.* **23**, 12892 (2017).
- ³⁰M. J. Frisch, G. W. Trucks, H. B. Schlegel, G. E. Scuseria, M. A. Robb, J. R. Cheeseman, G. Scalmani, V. Barone, G. A. Petersson, H. Nakatsuji, X. Li, M. Caricato, A. V. Marenich, J. Bloino, B. G. Janesko, R. Gomperts, B. Mennucci, H. P. Hratchian, J. V. Ortiz, A. F. Izmaylov, J. L. Sonnenberg, D. Williams-Young, F. Ding, F. Lipparini, F. Egidi, J. Goings, B. Peng, A. Petrone, T. Henderson, D. Ranasinghe, V. G. Zakrzewski, J. Gao, N. Rega, G. Zheng, W. Liang, M. Hada, M. Ehara, K. Toyota, R. Fukuda, J. Hasegawa, M. Ishida, T. Nakajima, Y. Honda, O. Kitao, H. Nakai, T. Vreven, K. Throssell, J. A. Montgomery, Jr., J. E. Peralta, F. Ogliaro, M. J. Bearpark, J. J. Heyd, E. N. Brothers, K. N. Kudin, V. N. Staroverov, T. A. Keith, R. Kobayashi, J. Normand, K. Raghavachari, A. P. Rendell, J. C. Burant, S. S. Iyengar, J. Tomasi, M. Cossi, J. M. Millam, M. Klene, C. Adamo, R. Cammi, J. W. Ochterski, R. L. Martin, K. Morokuma, O. Farkas, J. B. Foresman, and D. J. Fox, *GAUSSIAN 09*, Revision D.01, Gaussian, Inc., Wallingford, CT, 2013.
- ³¹W. Humphrey, A. Dalke, and K. Schulten, *J. Mol. Graphics* **14**, 33 (1996).
- ³²A. Ribar, S. E. Huber, M. A. Śmialek, K. Tanzer, M. Neustetter, R. Schürmann, I. Bald, and S. Denifl, *Phys. Chem. Chem. Phys.* **20**, 5578 (2018).
- ³³J. W. Ochterski, *Thermochemistry in Gaussian* (Gaussian, Inc., 2000), p. 1.
- ³⁴J. Simons, *Acc. Chem. Res.* **39**, 772 (2006).
- ³⁵D. E. Woon and T. H. Dunning, *J. Chem. Phys.* **100**, 2975 (1994).
- ³⁶M. Gutowski and J. Simons, *J. Chem. Phys.* **93**, 3874 (1990).
- ³⁷J. Rak, P. Skurski, and M. Gutowski, *J. Chem. Phys.* **114**, 10673 (2001).
- ³⁸M. Gutowski, K. D. Jordan, and P. Skurski, *J. Phys. Chem. A* **102**, 2624 (1998).
- ³⁹S. Denifl, B. Sonnweber, G. Hanel, P. Scheier, and T. D. Märk, *Int. J. Mass Spectrom.* **238**, 47 (2004).
- ⁴⁰H. Abdoul-Carime, M. A. Huels, E. Illenberger, and L. Sanche, *J. Am. Chem. Soc.* **123**, 5354 (2001).
- ⁴¹R. Abouaf, J. Pommier, and H. Dunet, *Int. J. Mass Spectrom.* **226**, 397 (2003).
- ⁴²R. Schürmann, T. Tsering, K. Tanzer, S. Denifl, S. V. K. Kumar, and I. Bald, *Angew. Chem., Int. Ed.* **56**, 10952 (2017).
- ⁴³R. Schürmann, K. Tanzer, I. Dąbkowska, S. Denifl, and I. Bald, *J. Phys. Chem. B* **121**, 5730 (2017).
- ⁴⁴J. Rackwitz, J. Kopyra, I. Dąbkowska, K. Ebel, M. L. Ranković, A. R. Milosavljević, and I. Bald, *Angew. Chem., Int. Ed.* **55**, 10248 (2016).
- ⁴⁵S. Ptasińska, S. Denifl, B. Mróz, M. Probst, V. Grill, E. Illenberger, P. Scheier, and T. D. Märk, *J. Chem. Phys.* **123**, 124302 (2005).
- ⁴⁶S. Ptasińska, S. Denifl, S. Gohlke, P. Scheier, E. Illenberger, and T. D. Märk, *Angew. Chem., Int. Ed.* **45**, 1893 (2006).
- ⁴⁷G. Hanel, B. Gstir, S. Denifl, P. Scheier, M. Probst, B. Farizon, M. Farizon, E. Illenberger, and T. D. Märk, *Phys. Rev. Lett.* **90**, 188104 (2003).
- ⁴⁸S. Ptasińska, S. Denifl, P. Candori, S. Matejcik, P. Scheier, and T. D. Märk, *Chem. Phys. Lett.* **403**, 107 (2005).
- ⁴⁹S. Denifl, H. D. Flosadóttir, A. Edtbauer, O. Ingólfsson, T. D. Märk, and P. Scheier, *Eur. Phys. J. D* **60**, 37 (2010).
- ⁵⁰X. Li, L. Sanche, and M. D. Sevilla, *J. Phys. Chem. A* **106**, 11248 (2002).
- ⁵¹J. B. Hendrickson and P. L. Skipper, *Tetrahedron* **32**, 1627 (1976).
- ⁵²S. Ptasińska, D. Gschliesser, P. Bartl, I. Janik, P. Scheier, and S. Denifl, *J. Chem. Phys.* **135**, 214309 (2011).
- ⁵³J. C. Rienstra-Kiracofe, G. S. Tschumper, H. F. Schaefer, S. Nandi, and G. B. Ellison, *Chem. Rev.* **102**, 231 (2002).
- ⁵⁴C. Desfrancis, *Phys. Rev. A* **51**, 3667 (1995).
- ⁵⁵R. A. Bachorz, J. Rak, and M. Gutowski, *Phys. Chem. Chem. Phys.* **7**, 2116 (2005).
- ⁵⁶P. D. Burrow, G. A. Gallup, A. M. Scheer, S. Denifl, S. Ptasińska, T. Märk, and P. Scheier, *J. Chem. Phys.* **124**, 124310 (2006).
- ⁵⁷S. Denifl, S. Ptasińska, G. Hanel, B. Gstir, M. Probst, P. Scheier, and T. D. Märk, *J. Chem. Phys.* **120**, 6557 (2004).
- ⁵⁸F. Ferreira da Silva, C. Matias, D. Almeida, G. Garcia, O. Ingólfsson, H. D. Flosadóttir, B. Ómarsson, S. Ptasińska, B. Puschnigg, P. Scheier, P. Limão-Vieira, and S. Denifl, *J. Am. Soc. Mass Spectrom.* **24**, 1787 (2013).
- ⁵⁹R. Balog, J. Langer, S. Gohlke, M. Stano, H. Abdoul-Carime, and E. Illenberger, *Int. J. Mass Spectrom.* **233**, 267 (2004).